EFECTO DEL TRATAMIENTO TÉRMICO SOBRE LA SOLUBILIDAD DEL HIDRÓGENO EN LA ALEACIÓN Zr-2.5Nb

EFFECT OF HEAT TREATMENT ON HYDROGEN SOLUBILITY IN Zr-2.5Nb ALLOY

C. García[1], V.P. Ramunni[*2,3] y G. Domizzi[1,3]

[1] *Instituto Sabato - UNSAM/CNEA, Av. Gral. Paz 1499, (1650) San Martín - Argentina.*
[2] *CONICET Godoy Cruz 2390 (C1425FQD) - Argentina.*
[3] *Gcia. Materiales-CNEA, Av. Gral. Paz 1499, (1650) San Martín - Argentina.*

Recibido: 02/06/2021; Aceptado: 24/12/2021

Estudiamos la solubilidad sólida terminal (SST) del hidrógeno (H) en muestras de Zr-2.5Nb tratadas térmicamente a 470°C duramte 10 h, seguidas de una carga gaseosa de hidrógeno y un tratamiento de homogeinización a 470°C durante 6 h para redistribuir el H en el volumen de la muestra. La microestructura fue caracterizada por microscopía óptica, microscopía electrónica de barrido y por rayos X. Ensayos de calorimetría diferencial fueron realizados para determinar las temperaturas de disolución y precipitación de hidruros. Nuestros resultados revelaron que comparativamente con los tratamientos a 380 °C realizados por otros autores, el tratamiento térmico aquí empleado no afecta significantemente la microestructura; no obstante la SST resultó ser ligeramente mayor.

Palabras clave: hidrógeno, hidruros, solubilidad, aleaciones Zr-2.5Nb, ensayos experimentales.

We have studied the hydrogen terminal solid solubility (TSS) on Zr-2.5Nb. The samples were aged at 470 °C for 10 h, plus a hydrogen gaseous charge followed by a homogenization treatment at 470 °C - 6 h in order of distributing the hydrogen throughout the sample's bulk. The microstructure was characterized by Optical Microscopy, Scanning Electron Microscopy, and X-Rays. Differential Scanning Calorimetry (DSC) test were carried out to determine the hydrides dissolution and precipitation temperatures from which the hydrogen TSS curves were obtained. Our results reveal that the thermal treatment employed has not significantly affected the microstructure compared to treatments at 380 °C by other authors; however, the hydrogen TSS was slightly higher.

Keywords: hydrogen, hydrides, solubility, Zr-Nb alloys, experimental tests

https://doi.org/10.31527/analesafa.2022.33.1.24 ISSN 1850-1168 (online)

I. INTRODUCTION

The Delayed Hydride Cracking phenomena (DHC), is a fracture mechanism which occurs in materials where hydrides are formed, as is the case of zirconium and its alloys. In the particular case of Zr-2.5Nb, which is used in the manufacture of the pressure tubes of CANDU type nuclear power plants, DHC can lead to the catastrophic rupture of the component. Hydrogen can be present as a remnant impurity of the manufacturing process or enter in the alloy during the material service life. It is very important to evaluate the alloy properties with the hydrogen concentration. The DHC phenomena [1] depends on the microstructure, the hydrogen solubility and the hydrogen diffusion. For example, Zr-2.5Nb is a bi-phasic alloy with grains in the α phase (hcp, with 0.6% Nb) surrounded by plates in the β-Zr phase (bcc, with 20% Nb). During thermal treatments, TT, the original plates of β-Zr lose continuity and the fast H-diffusion paths are interrupted while their Nb concentration changes [2]. Here we have studied the hydrogen's terminal solid solubility (TSS) for an intermediate temperature between the two thermal treatments performed by Parodi et al. [3] on Zr-2.5Nb. With this purpose we have submitted the samples to ageing, gaseous hydride charge and a homogenization thermal treatment; and characterized the microstructure and hydride structure by optical microscopy, scanning electron microscopy and X-rays. In order to obtain the hydrogen's TSS we have determined the hydride's dissolution (T_D) and precipitation (T_P) temperatures. The hydrogen Terminal Solid Solubility for Dissolution (TSSD) and Precipitation (TSSP) curves were measured by Differential Scanning Calorimetry (DSC). The present paper is structured as follows: Section II describes the hysteresis effect on the hydrogen solubility. Sections III and IV-VI, are devoted to summarize the material and the experimental treatments performed on the samples, respectively. Section VII summarizes our experimental results. The last section presents some conclusions.

II. HYDROGEN SOLUBILITY IN Zr BASED ALLOYS

Zirconium and its alloys show an important hysteresis between terminal solid solubility of hydrogen during heating or dissolution (TSSD) and cooling or precipitation (TSSP). This behavior has been ascribed to plastic deformation produced in a α-Zr matrix during hydride precipitation [1, 2] by the misfit between matrix and hydride. In two-phase Zr-2.5Nb alloy, TSS curves depend on the fraction and composition of both, α-Zr and β-Zr phases and also on thermal cycles [1]. Fig. 1 shows the Zr-H system pha-

* vpram@cnea.gov.ar

se equilibrium diagram [4] and the hydride compositions in Zr.

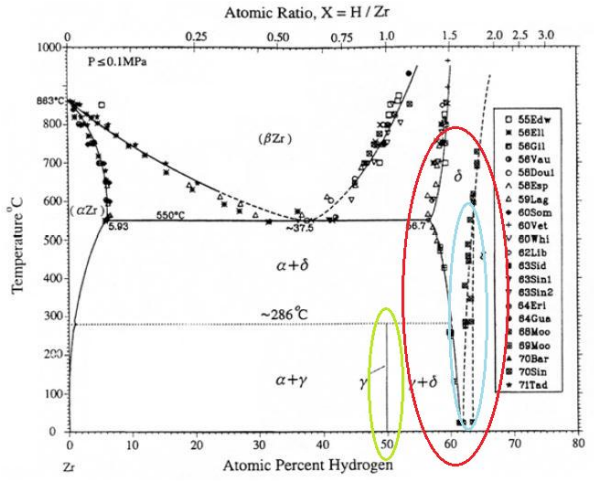

FIG. 1: Equilibrium phase diagram of the Zr-H system taken from Ref. [4].

The Terminal Solid Solubility (TSS) is defined as the maximal hydrogen concentration in solution without forming hydrides [5]. As shown in Fig. 2 [5], the TSS curve for hydrogen dissolution vs. temperature presents the hysteresis phenomenon for the heating and cooling processes. As the

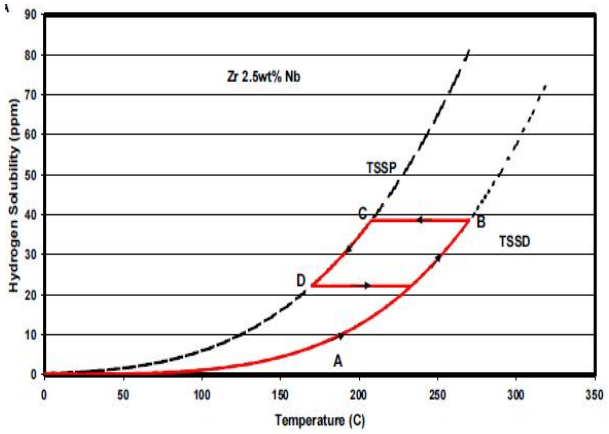

FIG. 2: Hydrogen solubility hysteresis effect in a thermal cycle on a Zr-2.5Nb sample [6].

temperature increases, the hydrogen concentration, C_H, in α-Zr increases following the TSSD dissolution curve along the segment AB. When the temperature decreases, BC, C_H does not change until the TSSP curve is reached (C point). When the temperature decreases, C_H decreases, segment CD. C_H does not change until the TSSD curve is reached. The hysteresis has been ascribed to plastic deformation produced in α-Zr matrix during hydride precipitation [6, 7] by the misfit between matrix and hydride. In two-phase Zr alloys, TSS curves depend on the fraction and composition of α and β phases [1, 2] and also on thermal cycles [8]. The TSSD and TSSP curves are obtained from the differential scanning calorimetry technique, DSC, which allows to determine the hydride's dissolution (T_D) and precipitation (T_P) temperatures. T_D has only one value, while T_P depends in general on the maximum temperature to which the sample was previously heated, the time at which that temperature is holding and the cooling speed [7].

III. MATERIAL AND Zr-2.5Nb SAMPLES

Zr2.5Nb samples come from a section of an extruded and cold worked pressure tube, autoclaved at 400 °C for 24 h, with approximate size of $(40 \times 30 \times 4.3)$ mm^3. These samples were prepared by an ageing thermal treatment, hydrogen charge and a homogenization treatment as described below. Table 1 summarizes the chemical composition of the samples.

TABLA 1: Samples chemical composition.

	Nb (%wt)	H (ppm)	O (ppm)
Sample	2.7 ± 0.1	16.1 ± 4.4	820 ± 82

The hydrogen TSS on samples of Zr-2.5Nb have been previously studied by Parodi et al. [3]. They have performed two thermal treatments, TT, namely: (i) 168 hours at 500°C and (ii) 24 hours at 380°C. These TT have resulted in the ageing of the β-Zr phase and in the increase of the Nb concentration up to 93 % and 59 %, respectively. We have here studied an intermediate TT between the two carried out in the work of Parodi [3] obtaining then a Nb concentration of 77 % in the β-Zr phase. Fig. 3 shows the Time-Temperature

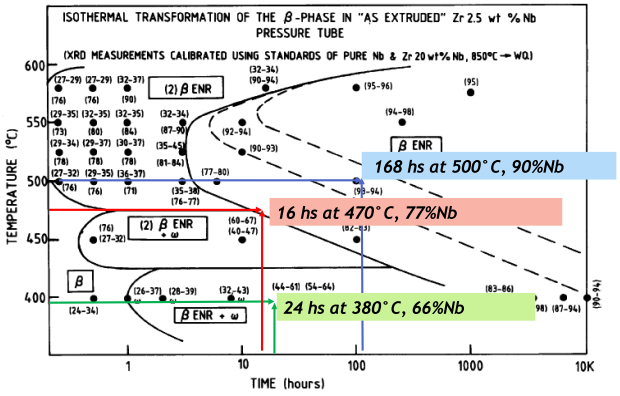

FIG. 3: Time-Temperature Transformation diagram of Zr-2.5 Nb [9].

transformation diagram of Zr-2.5 Nb [9]. The samples of $10 \times 10 \times 5$ mm^3, were treated at 470°C for 10 h in vacuum to decompose the β-Zr phase in order to produce a variation in the Nb concentration. After the ageing TT, the samples were polished to eliminate the superficial defects, and cleaned with trichlorethylene to remove all possible dirt on the sample surface. Afterwards, an electrolytic oxide film deposition with a 4 % SO_4H_2 solution was performed. The oxide film was then removed with a 600-grit silicon carbide paper, except on the edges of the surface. This anodizing process was carried out with the purpose of allowing the hydrogen enters into the sample during the gaseous charge only through the oxide free surfaces. Then, hydrogen diffuses homogeneously throughout the thickness of the sample. The process is shown in Fig. 4. Finally, the samples were submitted to a gaseous hydrogen charge procedure. Hy-

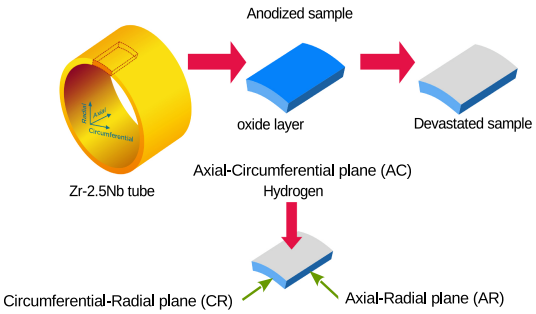

FIG. 4: Steps before the hydrogen gaseous charge process.

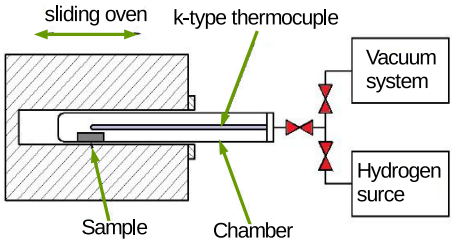

FIG. 5: Scheme of the gaseous hydrogen charge equipment.

drogen is incorporated into the sample using the SIEVERT equipment in the Fig. 5. The charging temperature was set at 350°C so that the oxide layer is not removed. The amount of hydrogen moles, n, which enters into the sample was calculated with the ideal gas equation, $PV = nRT$, by measuring the difference between the initial and final pressure, P, and the room temperature, T, V is the chamber volume and R the ideal gas constant.

TABLA 2: The total H concentration on samples, $C_H^T = C_H + C_H^0$, with C_H^0 the initial hydrogen concentration and the incorporated amount, C_H.

Sample	C_H	C_H^T
M_1	46	46 + 12 = 58
M_2	73	73 + 12 = 85
M_3	107	107 + 12 = 119
M_4	126	126 + 12 = 138

After the gaseous charge the hydrogen remains mostly on the sample surface. Since, it has no time enough to diffuse homogeneously a hydride gradient was generated through the sample thickness. Then, we perform a final TT at 470°C - 6 h for hydrogen homogenization. The maximum temperature reached and the duration of the treatment are factors that deserves some cares due to their importance regarding the transformation of the β-Zr phase during the ageing treatment.

IV. SAMPLES CHARACTERIZATION

In order to characterize the microstructure and hydride distribution the samples were observed by Optical Microscopy (OM) and Scanning Electron Microscopy (SEM). The microstructure was reveal by etching in a solution of 45 ml of nitric acid, 45 ml of distilled water and 6 ml of hydrofluoric acid, while a solution of 45 ml of nitric acid, 45 ml of lactic acid and 7 ml of hydrofluoric acid, to reveal the hydride particles. For a sample with 85 ppm of H, Figs. 6 and 7 show the micrograph obtained by SEM, on the Circumferential-Radial plane (CR) and on the Axial-Radial plane (AR), respectively. The presence of dark and light grey phases, correspond respectively to α- and β-Zr.

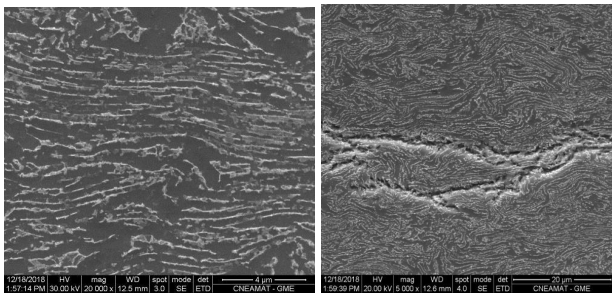

FIG. 6: (a) Left: SEM of the CR plane (see Fig. 4) of a sample with 85 ppm of H. (b) Right: The presence of hydride is emphasized.

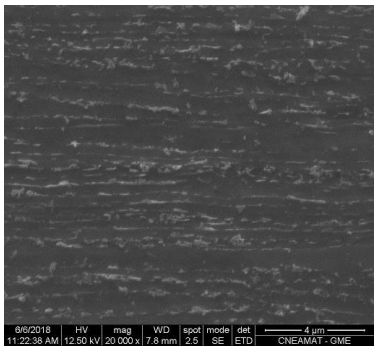

FIG. 7: SEM of the AR plane (see Fig. 4) of the same sample.

Fig. 8, shows the orientation and morphology of the hydrides precipitated on the CR plane of the pressure tube. In all cases, the hydrides form plates whose orientation is perpendicular to the radial direction. These so-called çircumferential"hydrides are oriented according to the crystalline texture and residual stresses of the tube. We have observed that, hydrides quantity and length increase with the hydrogen concentration.

V. X-RAY DIFFRACTION

X-ray diffraction tests were performed with a conventional diffractometer from the position $2\theta = 33.0°$ to $2\theta = 39.90°$; with a step of $0.01°$ and 33 seconds per time step, and Cu radiation. These initial parameters were used in order to observe the peak corresponding to the reflection on the (110) plane of the β phase. The degree of β-Zr phase transformation was evaluated through its Nb concentration by using Eq. (1), which correlates %at Nb with the lattice parameter a_β of the β-Zr phase [10]

$$a_\beta(\text{Å}) = 3.5878 - 0.00288 \times C_{Nb}(\%atNb). \quad (1)$$

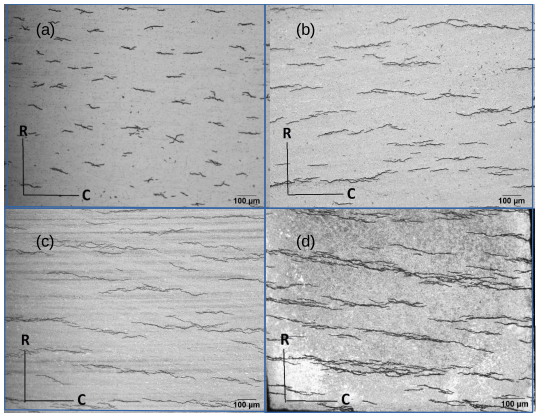

FIG. 8: Hydride distribution along the CR plane of samples heat treated at 470 ° 16 h, respectively with (a) 58, (b) 85, (c) 119 and (d) 138 ppm of H.

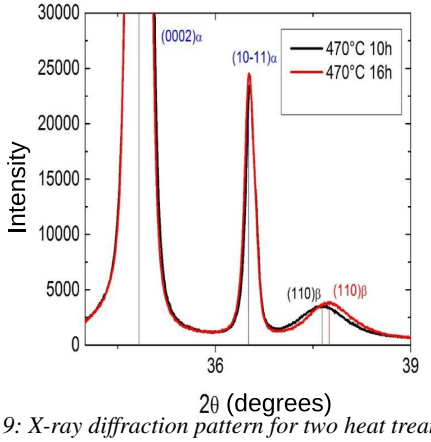

FIG. 9: X-ray diffraction pattern for two heat treatments.

VI. DIFFERENTIAL SCANNING CALORIMETRY

Differential Scanning Calorimetry (DSC) measurements were performed to obtain the hydride's dissolution, T_D, and precipitation, T_P, temperatures. The terminal solid solubility curves (TSSD/TSSP) are determined from T_D and T_P using the maximum slope temperature (MST) [3] criteria and the total hydrogen concentration. Before DSC measurements samples of approximately $2.5 \times 2.5 \times 4$ mm, were cleaned in ultrasonic bath containing acetone. All experiments were performed with an empty crucible as reference, under an Ar (99.9997 %) dynamic atmosphere of 25 ml/min. The equipment was calibrated using the melting point of In, Sn, Al, Fe elements. Each cycle consisted of a heating up to a maximum temperature (T_{max}), hold time at this temperature and cooling to a minimum temperature. Two runs were performed at $T_{max} = 380\,^{\circ}$C and two others at $T_{max} = 450\,^{\circ}$C in order to analyse the effect of the maximum temperature on T_P and to obtain TSSP2 and TSSP1, respectively. In these cycles, hold times at maximum temperatures were 10 min, with heating and cooling rates of 10 °C/min. Dissolution and precipitation temperatures result from the average of the values obtained after each T_{max}.

VII. EXPERIMENTAL RESULTS

X-Ray diffraction

Zr-2.5Nb X-ray diffraction patterns for two TT are shown in Fig. 9. The position of the (110)-β and (0002)- and (10$\bar{1}$1)-α peaks, are also presented.

In Table 3 we summarize the values of a_β parameter and Nb concentration of the β-Zr phase according to the according to the thermal treatment performed.

TABLA 3: Lattice parameter, a_β, and Nb concentration in β-Zr phase according to the thermal treatment.

T.T. (°C/h)	a_β (Å)	%Nb (%at)	%Nb (%wt)
470 - 10	3.377	73.0	73.4
470 - 16	3.367	76.3	76.6
380 - 24	3.397	66.1	66.5
500 - 168 [3]	3.319	93.1	93.2

Thermal solid solubility curves (TSS)

Table 4 shows the results obtained from the heating and cooling calorimetry curves. It lists the total hydrogen concentration C_H (in weight ppm), the dissolution temperatures T_D for both, γ and δ, hydrides and the precipitation temperature for delta hydrides (T_P) with different maximum temperatures. The first heating cycle corresponds to the dissolution of hydrides precipitated during cooling carried out after the homogenization treatment. In this cycle, samples with 85 and data 118 ppm of H present two dissolution peaks, one of γ-hydrides and another of δ-hydrides. For 58 ppm the sensitivity of DSC could not be enough to detect the minority γ phase. Regarding the sample wit 138 ppm the γ-hydride was not detected either; in Ref. [11] was observed that the precipitation of the γ-hydride decreases as the hydrogen concentration increases. The γ-hydrides were no detected during the subsequent DSC cycles of heating and cooling with a rate of 10 °C/min. This may be due to the fact that the γ-hydride precipitates by a peritectoid transformation, as reported in Ref. [11, 12], thus a cooling rate lower than 10 °C/min is required. Hydrogen Terminal Solid Solubility for Dissolution (TSSD) and Precipitation (TSSP) curves were calculated by fitting the hydrogen concentration C_H versus T_D/T_P of δ-hydrides reported in Table 4, according to the Arrhenius equation (2),

$$C_H = C_0 \exp(-\frac{Q_{D,P}}{RT}). \quad (2)$$

Where C_0 is the pre-exponential factor, $Q_{D,P}$, are the transformation hydrides enthalpy for dissolution or precipitation respectively, and R is the gas constant. C_0 and $Q_{D,P}$ varies according to the alloy and the hydride phase. So, three equations can be obtained, for dissolution (3) and for precipitation (4), where i=1 corresponds to $T_{max} = 450\,^{\circ}$C and $i = 2$ to $T_{max} = 380\,^{\circ}$C.

$$TSSD = C_0 \exp(-\frac{Q_D}{RT}), \quad (3)$$

$$TSSP_i = C_0 \exp(-\frac{Q_{P_i}}{RT}). \quad (4)$$

The enthalpy of dissolution, Q_D, and precipitation, Q_{P_i}, are expressed as,

$$Q_D = Q_q - w_{el,D} + w_{pl,D} + w_{int,D}, \quad (5)$$

$$Q_P = Q_q + w_{el,P} + w_{pl,P} + w_{int,P}. \quad (6)$$

In Eqs. (5) and (6), Q_q is the chemical energy, W_{el} and W_{pl} the elastic and plastic energies associated with the mismatch between hydride and matrix (due to the difference in specific volume between both phases), and W_{int} the interaction energy with the stresses in the environment of the hydride (such as residual stresses, applied external stresses and stresses between the microplates). The term $W_{pl,D}$ implies that the plastic deformation produced during hydride precipitation is recovered, which depends on the temperature attained during heating. Fig. 10 displays the experimental data reported in Table 4 and the TSSD, TSSP1 and TSSP2 curves. For samples with 58 and 138 ppm of H, no precipitation signal was detected during the cooling cycle from $T_{max} = 380\,^{\circ}$C, so the TSSP2 curve could not be obtained with more data. Table 5 shows the adjustment parameters for each curve with and without considering the hydrogen concentration of 58 ppm.

Sample	C_H (ppm)	Cicle	T_{max}	T_D γ	T_D δ	T_{max}	T_P δ
1	58	1	470	-	-	380	-
		2	380	-	-	380	-
		3	380	-	-	450	-
		4	450	-	226	450	164
2	85	1	470	204	318	380	255
		2	380	-	310	380	254
		3	380	-	313	450	238
		4	450	200	310	450	236
3	119	1	470	243	279	380	283
		2	380	.	340	380	284
		3	380	-	336	450	265
		3	450	-	-	450	264
4	138	1	470	-	-	380	-
		2	380	-	-	380	-
		3	380	-	375	450	308
		4	450	-	377	450	308

TABLA 4: The precipitation and dissolution temperatures, T_P, T_D for different H concentrations at a heating/cooling rate of 10°C/min.

TABLA 5: Parameters obtained from the fit with/without $C_H = 58ppm$.

Parameters	**TSSD**	**TSSP1**
A (ppm)	3300 / 6951	2300 / 3410
Q (J/mol)	16967 / 20785	13631 / 15396

Fig. 11 includes TSSD results of this work together with those measured by Parodi et al., [3] with different thermal treatments. In Ref. [3], the samples with 93.1 % at Nb in β-phase (treated at 500°C - 168 h) showed a lower TSS than the samples with 66.1 % at of Nb (treated at 380°C - 24 h). It was expected that the material treated at 470°C with

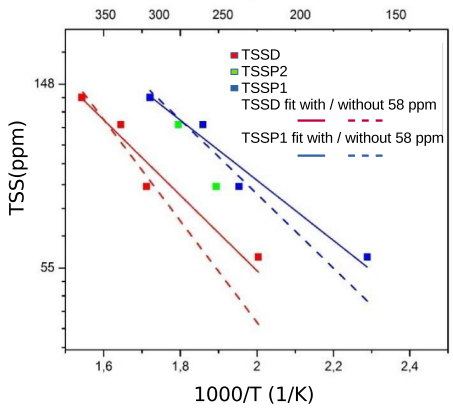

FIG. 10: Hydrogen concentration C_H and dissolution/precipitation temperatures reported in Table 4. The fitting lines were obtained with the Arrhenius equation (2).

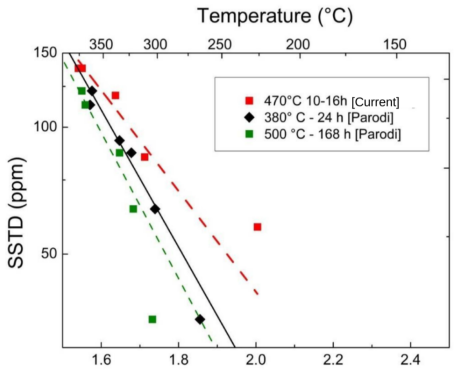

FIG. 11: Comparison of the TSSD δ-hhydride results measured in this work and those reported in ref 3, with thermal treatments at three different temperatures.

76.3 % Nb in β-phase would have an intermediate solubility between the two treatments evaluated by Parodi since the beta phase contains an intermediate percentage of Nb. Nevertheless, its TSSD is higher as shown in Fig.11. On the other hand, Müller [13] used the material treated at 380°C - 24 h and measured the solubility after a quenching treatment and thermal cycling with heating / cooling rates of 10°C/min. He have found that, although the β phase has the same ageing before and after quenching, the solubility of hydrogen is affected by the different distribution of hydrides, this result was interpreted by means of the Eqs. (5) and (6). The quenching treatment promotes a finer hydride distribution, which means that they retain greater elastic deformation, thus reducing the value of Q and increasing the TSSD and TSSP. Figs. 12 and 13 show our TSSD, TSSP1 fitted curves with cooling of 10°C/min and those obtained by Müller [13] and Parodi [3].

Fig. 14(a) and (b), show the microstructure and hydride distribution for respectively 119 and 122 ppm of H in samples of Parodi [3] for TT at 380°C - 24 h and 500°C - 168 h. The continuity of the β phase treated at 470°C in this paper (Fig. 6(a)) is similar to that of the material treated at 380°C, while at 500°C the β phase is remarkably spheroidized. Thus the increment in TSS observed in the sam-

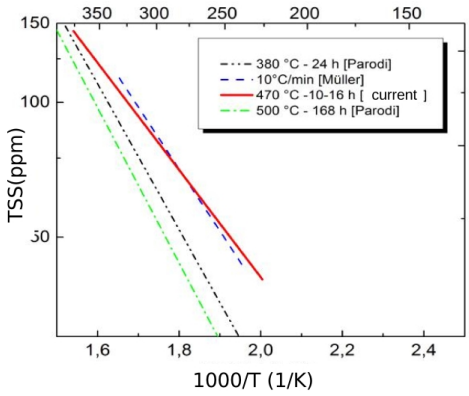

FIG. 12: Comparison of TSSD curves from present experiments with those obtained in [3, 13].

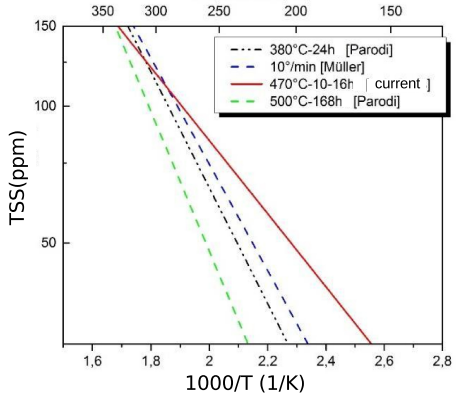

FIG. 13: Comparison of TSSP1 curves from present experiments with those obtained in [3, 13].

ples treated at 470°C could not be attributed to the β phase ageing. On the other hand, the hydride distribution observed in the samples of Parodi [3] is similar to that obtained in the sample with 119 ppm used in this work (Fig. 14(c)). So the unexpected higher TSS obtained with the TT at 470°C cannot be explained nor by the beta phase ageing neither by hydride distribution as it is observed by optical microscopy.

In Zirconium pressure tubes, hydride precipitates observed with low magnification are usually depicted like plates resting on the circumferential - axial plane, the so called circumferential hydrides. But, electron microscopy studies reveal that these plates are compose of stacks of smaller particles with habit plane $(111)_\delta$ close to the α-Zr basal plane $(0002)_\alpha$ [6]. More recent studies with X- Rays Synchrotron show that, the majority of δ particles precipitate in α-Zr grains having $(0002)_\alpha$ poles tilted 20 - 30 degrees from circumferential direction of the tube, and a minor fraction parallel to the circumferential (hoop) direction [14, 15]. This trend can be reverted by tensile stresses applied along hoop direction [14] or fast cooling rates [13, 15]. Under these conditions Terminal Solid Solubility increases [13, 14]. As inferred from Eqs. (5) and (6), several factors affects the hydride precipitation, the solubility of present phases, the ductility of the alloy, the presence of internal (such as intergranular) or external stresses. More studies are necessary, such as electron microscopy and X Ray synchrotron

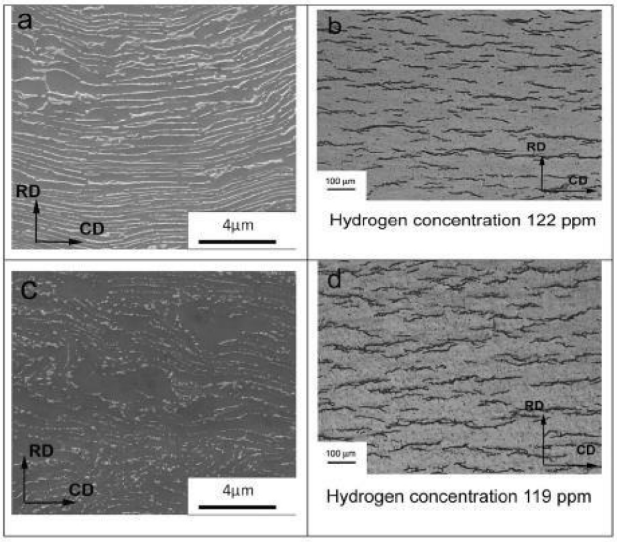

FIG. 14: Microstructure and hydride distribution of Zr-2.5Nb with (a)-(b) 122 ppm of H and (c)-(d) 119 ppm of H, respectively in Ref. [3].

or neutron diffraction, to clarify the result obtained in this work.

VIII. CONCLUSIONS

In summary, we have performed heat treatment on a Zr-2.5Nb pressure tube samples to be compared with other heat treatments reported in literature. Experimentally, the percentage of Nb in the beta phase was analysed and the dissolution / precipitation solubility of hydrogen in the alloy was calculated by differential scanning calorimetry tests.

Our experimental remarks are:

- Thermal treatment carried out at 470°C for 10 - 16 hours does not significantly affect the continuity of beta phase filaments compared to that of the same material treated at 380°C - 24 hours of Parodi [3] unlike the treatment at 500°C in which the β phase is spheroidized. A percentage of 73-77 % Nb in phase β was measured.
- The following curves were calculated for terminal solid solubility of dissolution and precipitation: $TSSD = 3300\exp(-16867.3/RT$ and $TSSP1 = 2300\exp(-13630.5/RT)$.
- Contrary to our expectative the TSS of the 470°C treatment is slightly higher than the measurements for the 380°C treatment.

ACKNOWLEDGEMENTS

This work was partially financed by CONICET PIP-11220170100021CO.

REFERENCES

[1] D. Khatamian. Solubility and partitioning of hydrogen in metastable Zr-based alloys used in the nuclear industry. J. Alloys Compd. **293-295,** 893-899 (1999).

[2] D. Khatamian. Effect of β-Zr decomposition on the solubility limits for H in Zr-2.5Nb. J. Alloys Compd. **356-357,** 22-26 (2003).

[3] S. A. Parodi, L. M. Ponzoni, M. E. D. L. Heras, J. I. Mieza y G. Domizzi. Study of variables that affect hydrogen solubility in α+β Zr-alloys. J. Nucl. Mater. **477,** 305-317 (2016).

[4] E. Zuzek, J. Abriata, A. San-Martin y F. Manchester. H-Zr(hydrogen-zirconium). Phase Diagrams of Binary Hydrogen Alloys, 309-322 (2000).

[5] R. Singh, S. Mukherjee, A. Gupta y S. Banerjee. Terminal solid solubility of hydrogen in Zr-alloy pressure tube materials. J. Alloys Compd. **389,** 102-112 (2005).

[6] V. Perovic, G. Weatherly y C. Simpson. Hydride precipitation in α/β zirconium alloys. Acta Metallurgica **31,** 1381-1391 (1983).

[7] D. Khatamian y V. Ling. Hydrogen solubility limits in α- and β-zirconium. J. Alloys Compd. **253-254,** 162-166 (1997).

[8] IAEA-TECDOC-1609. *Intercomparison of Techniques for Inspection and Diagnostics of Heavy Water Reactor Pressure Tubes: Determination of Hydrogen Concentration and Blister Characterization* (International Atomic Energy Agency, Viena, 2009).

[9] S. Aldridge y B. Cheadle. Age hardening of Zr-2.5 wt % Nb slowly cooled from the $(\alpha + \beta)$ phase field. J. Nucl. Mater. **42,** 32-42 (1972).

[10] G. Aurelio, A. F. Guillermet, G. J. Cuello y J. Campo. Structural properties and high-temperature reactions of the metastable Ω phase in Zr-Nb alloys. J. Nucl. Mater. **341,** 1-11 (2005).

[11] D. O. Northwood y D. T. Lim. A TEM metallographic study of hydrides in a Zr-2.5wt %Nb alloy. Metallography **14,** 21-35 (1981).

[12] S. Mishra, K. Sivaramakrihnan y M. Asundi. Formation of the gamma phase by a peritectoid reaction in the zirconium-hydrogen system. J. Nucl. Mater. **45,** 235-244 (1972).

[13] S. Müller, M. D. L. Heras, S. Alcántar, M. Luppo y J. Mieza. Hydrogen redistribution during hydride precipitation in Zr-2.5Nb pressure tubes. J. Nucl. Mater. **543,** 152544 (2021).

[14] P. Vizcaíno, J. Santisteban, M. V. Alvarez, A. Banchik y J. Almer. Effect of crystallite orientation and external stress on hydride precipitation and dissolution in Zr2.5 %Nb. J. Nucl. Mater. **447,** 82-93 (2014).

[15] O. V. Shiman, E. Tulk y M. R. Daymond. Synchrotron X-ray diffraction study of zirconium hydride distribution in Zr-2.5 %Nb and its redistribution during thermal cycling. Mater. Charact. **136,** 183-195 (2018).